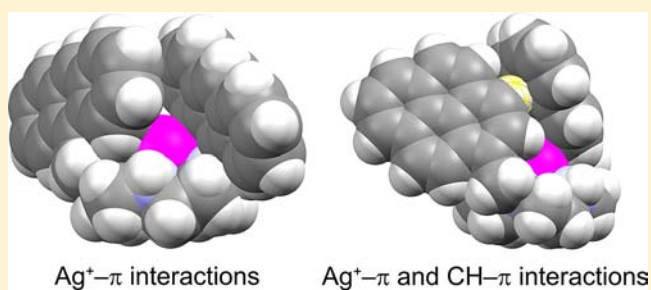


Argentivorous Molecules Bearing Two Aromatic Side-Arms: $\text{Ag}^+-\pi$ and $\text{CH}-\pi$ Interactions in the Solid State and in SolutionYoichi Habata,^{*,†,‡} Aya Taniguchi,[†] Mari Ikeda,^{†,‡} Takao Hiraoka,[†] Noriko Matsuyama,[†] Sakiko Otsuka,[†] and Shunsuke Kuwahara^{†,‡}[†]Department of Chemistry, Faculty of Science, and [‡]Research Center for Materials with Integrated Properties, Toho University, 2-2-1 Miyama, Funabashi, Chiba 274-8510, Japan

Supporting Information

ABSTRACT: Seven double-armed cyclens bearing two aromatic side-arms, at the 1- and 7-positions of the cyclens, were prepared via three steps from dimethyl 2,2'-iminodiacetate. The X-ray structures of the Ag^+ complexes and Ag^+ -ion-induced ^1H NMR spectral changes suggest that the two aromatic side-arms cover the Ag^+ ions incorporated in the ligand cavities, as if the aromatic ring “petals” catch the Ag^+ ions in the way a real insectivorous plant (Venus flytrap) catches insects, using two leaves. It is also reported that the $\text{CH}-\pi$ interactions between the aromatic side-arms, as well as the $\text{Ag}^+-\pi$ interactions, are crucial for double- and tetra-armed cyclens to work as argentivorous molecules.



INTRODUCTION

Increasing attention has been focused on metal-cation- π^1 and $\text{CH}-\pi^{2a-c}$ interactions. It is well known that weak molecular forces such as cation- π , $\text{CH}-\pi$, hydrogen-bonding, and dipole-dipole interactions are important for controlling the shapes of compounds and play a vital role in various specific phenomena in chemistry and biochemistry.^{2d} Recently, we reported that tetra-armed cyclens with aromatic side-arms behave like an insectivorous plant (Venus flytrap) when they form complexes with Ag^+ ions; that is, the aromatic side-arms cover the Ag^+ ions incorporated in the ligand cavities by $\text{Ag}^+-\pi$ interactions,³ and no conformational changes are observed when other metal cations are added in organic solvents or in water.^{4a,b} Several groups have reported the X-ray structures of Co^{2+} , Ni^{2+} , Cu^{2+} , and Zn^{2+} complexes with tetra-armed cyclens.⁵ Aromatic side-arms in the complexes with armed cyclens, however, never cover the metal ions incorporated in the cyclen unit. We therefore called the tetra-armed cyclens “argentivorous molecules”.⁶

The Venus flytrap uses two leaves to trap insects, so we prepared armed cyclens bearing two aromatic side-arms, at the 1- and 7-positions of the cyclen, to see if the armed cyclens behave like flytraps. Here we report that both $\text{Ag}^+-\pi$ and $\text{CH}-\pi$ interactions are important for tetra-armed cyclens and double-armed cyclens to act as argentivorous molecules.

RESULTS AND DISCUSSION

Double-armed cyclens (1a–7a in Figure 1) bearing two aromatic rings, at the 1- and 7-positions of the cyclen, were prepared via two steps from 1,4,7,10-tetraazacyclododecane-2,6-dione (see scheme in the Supporting Information).⁷

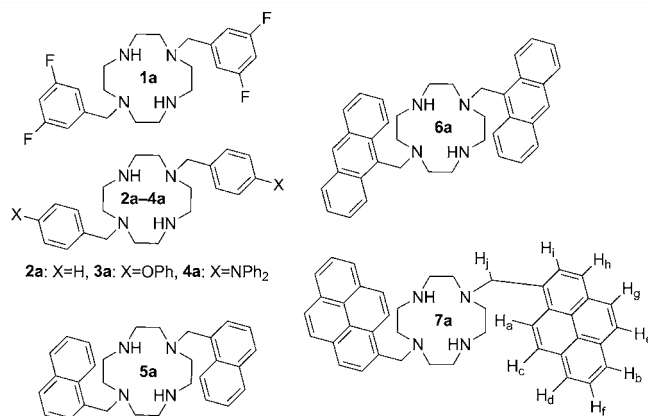


Figure 1. Double-armed cyclens.

AgCF_3SO_3 complexes were prepared using these new double-armed cyclens.

To compare the electron densities on the aromatic ring components we used, electrostatic potentials were calculated using the HF/6-31G(*) method.⁸ The electrostatic potential is defined as the energy of interaction of a positive point charge with the nuclei and electrons of a molecule, and the value of the electrostatic potential correlates with the electron densities on the aromatic rings. Figure 2 shows the electrostatic potential maps of the side-arm components of 1a–7a.⁹ Toluene (b) has the highest electrostatic potential of the benzene derivatives

Received: November 16, 2012

Published: February 13, 2013

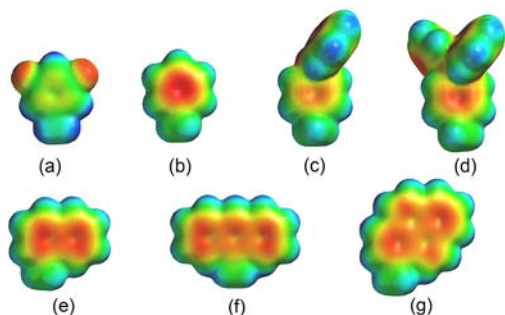


Figure 2. Electrostatic potential maps of (a) 1,3-difluoro-4-methylbenzene, (b) toluene, (c) 1-methyl-4-phenoxybenzene, (d) 4-methyl-*N,N*-dimethylaniline, (e) 1-methylnaphthalene, (f) 1-methylantracene, and (g) 1-methylpyrene.

(a–d in Figure 2). The electrostatic potentials of 1-methylnaphthalene (e), 1-methylantracene (f), and 1-methylpyrene (g) are higher than those of the substituted benzenes (a–d), and the areas with high electrostatic potentials are larger than those of the benzenes. We therefore expected that significant intramolecular $\text{Ag}^+ - \pi$ interactions would be observed in the double-armed cyclens with toluene (2a), 1-methylnaphthalene (5a), 1-methylantracene (6a), and 1-methylpyrene (7a) as side-arms.

Figure 3 shows the X-ray structure of the 2a/ AgCF_3SO_3 complex (see also Figure S4 in the SI for the X-ray structures of

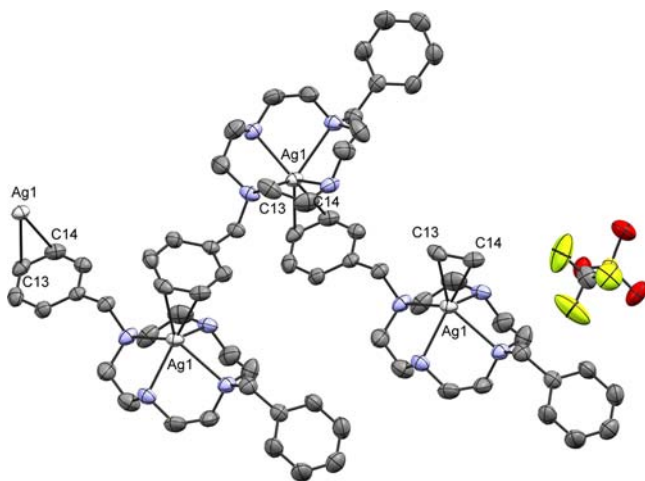


Figure 3. ORTEP diagram of the 2a/ AgCF_3SO_3 complex. Hydrogen atoms are omitted.

the 1a/ AgCF_3SO_3 and 3a/ AgCF_3SO_3 complexes). In the 2a/ AgCF_3SO_3 complex, the Ag^+ ion is coordinated by the four N atoms of the cyclen. Contrary to our expectations, the Ag^+ ion incorporated in the cyclen ring is not covered by the intramolecularly linked side-arms, but is covered by an aromatic side-arm of the nearest-neighbor molecule, resulting in the formation of the one-dimensional polymeric chain structure. The C13–Ag1 and C14–Ag1 distances are 2.608 and 2.577 Å, respectively.

In contrast, the side-arms in 4a, with triphenylamino groups, cover the Ag^+ ions in the ligand cavities (Figure 4). We confirmed $\text{Ag}^+ - \pi$ interactions between the aromatic side-arms and the Ag^+ ions because the C11–Ag1 and C30–Ag1 distances are 2.666 and 3.390 Å, respectively (in tetra-armed cyclens, typical C–Ag distance range is 3.272–3.344 Å^{4a}). In

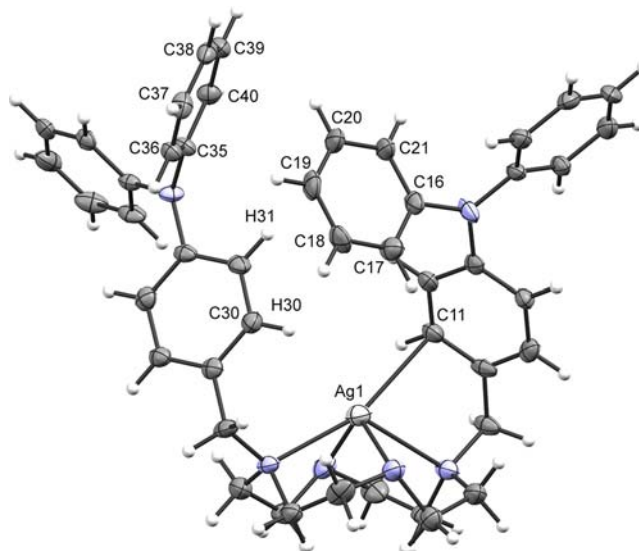


Figure 4. ORTEP diagram of the 4a/ AgCF_3SO_3 complex. CF_3SO_3^- and solvent are omitted.

this complex, the C11–Ag1 distance is shorter than the C30–Ag1 distance. Interestingly, intramolecular CH– π interactions between the aromatic rings are also observed in the 4a/ AgCF_3SO_3 complex. The H20–benzene plane (C35 to C40), H19–benzene plane (C35 to C40), H30–benzene plane (C16 to C21), and H31–benzene plane (C16 to C21) distances are 2.764, 2.791, 2.939, and 3.132 Å, respectively. The distances are comparable with typical CH– π distances in aromatic rings.^{2a,d}

On the other hand, in the 5a/ AgCF_3SO_3 and 6a/ AgCF_3SO_3 (Figure 5a–d) complexes, two side-arms cover the Ag^+ ions incorporated in the ligand cavities as if the two aromatic ring “petals” caught the Ag^+ ions in the way an insectivorous plant (Venus flytrap) catches insects, using two leaves. The C14–Ag1 distance in the 5a/ AgCF_3SO_3 complex and the C12–Ag1 and C27–Ag1 distances in the 6a/ AgCF_3SO_3 complex are 2.821, 2.753, and 2.863 Å, respectively. In these complexes, the $\text{Ag}^+ - \pi$ bond distances are shorter than those of the tetra-armed cyclens.

The conformation of the pyrene side-arms in the 7a/ AgCF_3SO_3 complex (Figure 6) is slightly different from those of the side-arms in the 5a/ AgCF_3SO_3 and 6a/ AgCF_3SO_3 complexes, although the two side-arms in the ligand cover the Ag^+ ion incorporated in the ligand cavity. The C4–Ag1, C5–Ag1, C53–Ag1, and C55–Ag1 distances are 2.633, 2.996, 3.113, and 3.387 Å, respectively. In the complex, the C4–Ag1 and C5–Ag1 distances are shorter than the C53–Ag1 and C55–Ag1 distances. The dihedral angle between the two pyrene planes is ca. 78°, whereas the dihedral angles between the two aromatic ring-planes in the 5a/ AgCF_3SO_3 and 6a/ AgCF_3SO_3 complexes are ca. 30°. As shown in Figure 6a and b, the H51–pyrene-plane and H61–pyrene-plane distances are 2.424 and 2.815 Å, respectively. These bond distances indicate CH– π interactions between two pyrenes.

In contrast, no side-arms cover the metal cations incorporated in the ligand cavities in the 6a/ HgCl_2 and 7a/ $\text{Cu}(\text{CF}_3\text{SO}_3)_2$ complexes (Figure 7). These X-ray structures suggest that (i) the aromatic rings that have higher electron densities, such as naphthalene, anthracene, and pyrene, cover the Ag^+ ions by $\text{Ag}^+ - \pi$ interactions, (ii) the side-arms cover the Ag^+ ions using $\text{Ag}^+ - \pi$ and CH– π interactions only when

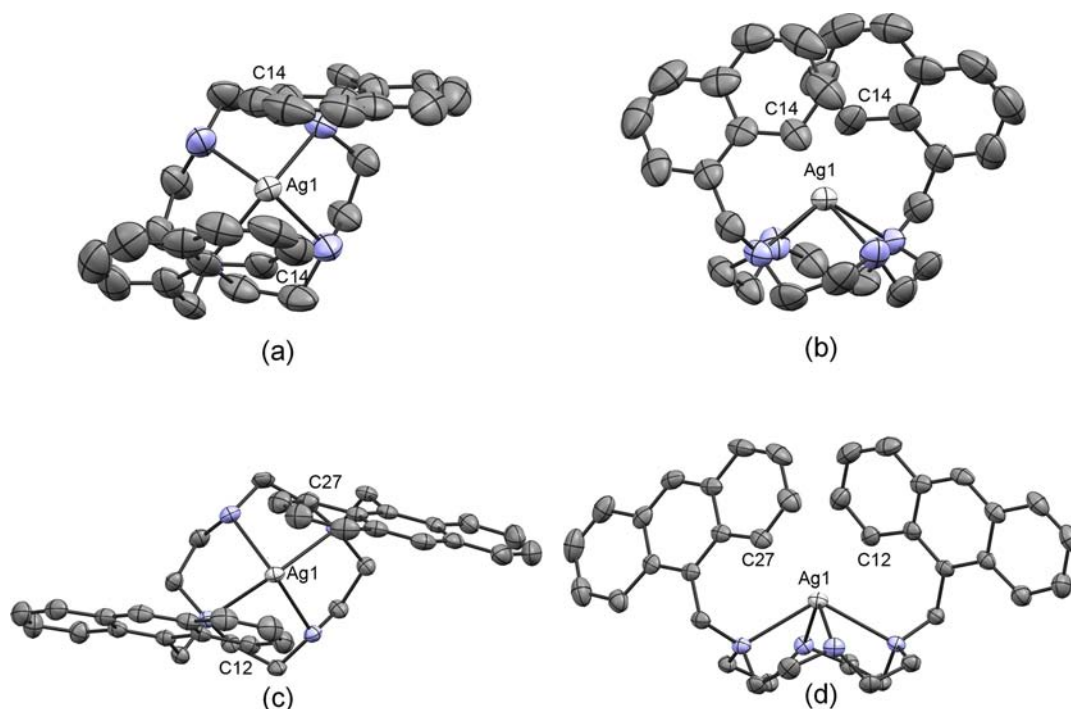


Figure 5. ORTEP diagrams of **5a**/ AgCF_3SO_3 [(a) top and (b) side views] and **6a**/ AgCF_3SO_3 [(c) top and (d) side views] complexes. Hydrogen atoms and CF_3SO_3^- are omitted.

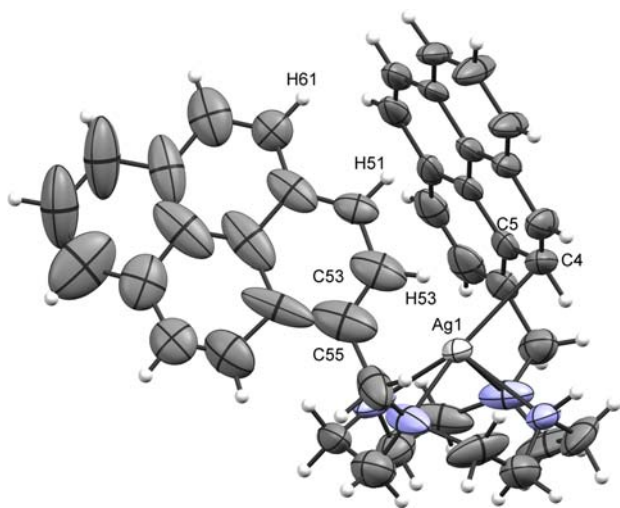


Figure 6. ORTEP diagrams of **7a**/ AgCF_3SO_3 . CF_3SO_3^- is omitted.

substituted benzenes that can participate in $\text{CH}-\pi$ interactions between the side-arms are introduced, and (iii) when pyrene is used as the side-arms, both $\text{Ag}^+-\pi$ and $\text{CH}-\pi$ interactions are observed. We previously reported that tetra-armed cyclens with four 4-nitrobenzenes, which have very low electron densities on the benzenes, act as argentivorous molecules. These findings suggest that $\text{CH}-\pi$ interactions, as well as $\text{Ag}^+-\pi$ interactions, play a crucial role in the behavior of argentivorous molecules.³

To determine the structures of the complexes in solution, Ag^+ -ion-induced ^1H NMR spectral changes were examined. As shown in Figure 8, upon addition of AgCF_3SO_3 (below 1.0 equiv), two sets of signals appeared (one for free **7a** and the second for its complex, primed), reflecting a slow-exchanging process. The complex signals (H_g' , H_h' , and H_i' protons in Figure 7) appear at higher field, ca. -0.12 , -0.49 , and -0.16

ppm, than the corresponding signals (H_g , H_h , and H_i protons) of free **7a**, respectively, upon addition of 1.0 equiv of Ag^+ ions. In contrast, in ^1H NMR titration experiments using **1a**, **2a**, and **3a**, no higher-field shifts of the aromatic protons were observed (see Figure S5 in the SI). These results indicate that the H_g , H_h , and H_i protons are located in the shielding area in another pyrene ring. In the X-ray structure of the **7a**/ AgCF_3SO_3 complex (Figure 6), the H_{61} , H_{53} , and H_{51} hydrogens corresponding to the H_g , H_h , and H_i protons are located in the shielding area of another pyrene ring. Both the ^1H NMR and X-ray data therefore strongly support the suggestion that the structure of the **7a**/ AgCF_3SO_3 complex in solution is similar to the solid-state structure.

To visualize the $\text{Ag}^+-\pi$ interactions, the isosurfaces of the LUMO and HOMO of the Ag^+ complexes were calculated using the B3LYP/3-21G(*) theoretical level.⁸ Figure 9 shows the LUMO (mesh) and HOMOs (solid) of the X-ray structures of the **4a**/ Ag^+ –**7a**/ Ag^+ complexes. In all cases, the LUMO of the Ag^+ ion is distorted by interaction with the HOMOs of the aromatic side-arms. These graphics clearly support $\text{Ag}^+-\pi$ interactions between the Ag^+ ion and the aromatic side-arms.

In conclusion, we demonstrated that double-armed cyclens bearing two aromatic side-arms with high electron densities behave like an insectivorous plant (Venus flytrap) by $\text{Ag}^+-\pi$ interactions. It was also shown that $\text{CH}-\pi$ interactions between aromatic side-arms, as well as the $\text{Ag}^+-\pi$ interactions, are crucial for double- and tetra-armed cyclens to work as argentivorous molecules. Applications of double-armed cyclens bearing chromophores (anthracene and pyrene) as metal-ion sensors are now in progress.

EXPERIMENTAL SECTION

General Information. Melting points were obtained with a Mel-Temp capillary apparatus and were not corrected. FAB mass spectra were obtained using a JEOL 600 H mass spectrometer. ^1H NMR spectra were measured in CDCl_3 on a JEOL ECP400 (400 MHz)

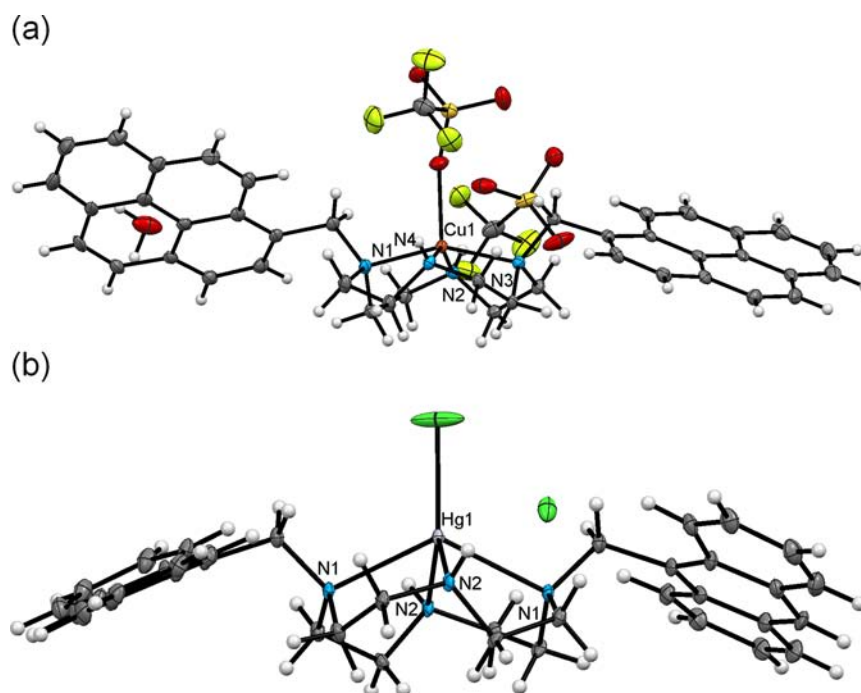


Figure 7. ORTEP diagrams of 7a/Cu(CF₃SO₃)₂ (a) and 6a/HgCl₂ (b).

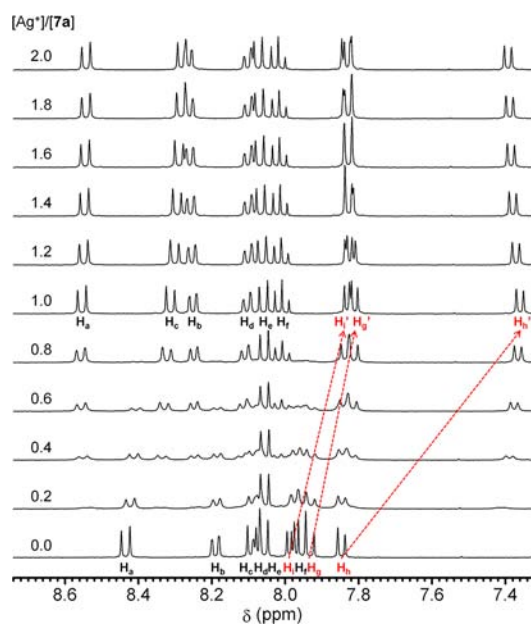


Figure 8. Ag⁺-ion-induced ¹H NMR spectral changes of 7a (in CD₂Cl₂/CD₃OD). The positions of the H_g, H_i, and H_j protons were assigned using ROESY, COSY, and 1D NOE NMR (Figure S6 in the SI).

spectrometer. Cold ESI-mass spectra were recorded on a JEOL JMS-T100CS mass spectrometer. Cyclen was purchased from Macrocylics. All reagents were standard analytical grade and were without further purification.

Preparation of 1,4,7,10-Tetraazacyclododecane-2,6-dione. 1,4,7,10-Tetraazacyclododecane-2,6-dione was prepared according to the procedure described in the literature. Yield: 32%. Mp: 168.0–169.0 (dec). ¹H NMR (D₂O): δ 3.64 (t, *J* = 5.5 Hz, 4H), 3.61 (s, 4H), 2.99 (t, *J* = 5.5 Hz, 4H). FAB-MS (*m/z*) (matrix: DTT/TG = 1:2): 201 ([*M* + 1]⁺, 100%).

General Procedures for the Reaction of Cyclen-dione with Aromatic Aldehydes. After stirring a mixture of cyclen-dione (10.0

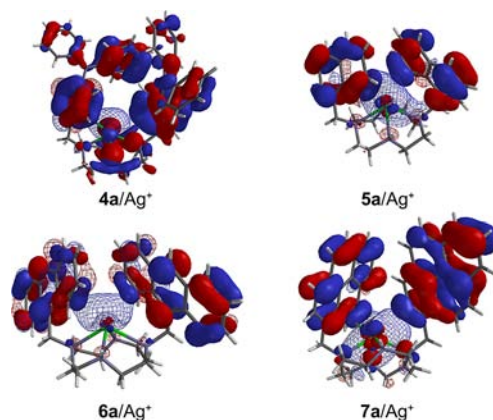


Figure 9. LUMOs and HOMOs calculated by the DFT methods [B3LYP/3-21G(*)] using the X-ray structures of the Ag⁺ complexes with 4a–7a (isosurface value is 0.032 au). 4a/Ag⁺ complex, LUMO[+1] (mesh) and HOMO[-10] (solid); 5a/Ag⁺ complex, LUMO[+4] (mesh) and HOMO[-3] (solid); 6a/Ag⁺ complex, LUMO[+4] (mesh) and HOMO[-1] (solid); 7a/Ag⁺ complex, LUMO[+5] (mesh) and HOMO[-2], HOMO[-6] (solid).

mmol) and 3,5-difluorobenzaldehyde (35.2 mmol) in dry 1,2-dichloroethane (100 mL) at room temperature for 1 day under an argon atmosphere (1 MP), NaBH(OAc)₃ (35.1 mmol) was added and the mixture was stirred for 1 day at room temperature. Saturated aqueous NaHCO₃ was added, and the aqueous layer was extracted with chloroform three times. The combined organic layer was washed with water, dried over Na₂SO₄ and concentrated. The residual solid was recrystallized from acetonitrile to give 1b in 93% yield. Mp: 138.4–139.2 °C. ¹H NMR (CDCl₃): δ 6.97–6.91 (m, 2H), 6.93–6.85 (m, 4H), 6.82–6.74 (m, 2H), 3.89 (s, 2H), 3.69 (s, 2H), 3.30 (q, *J* = 5.6 Hz, 4H), 3.27 (s, 4H), 2.62 (t, *J* = 5.6 Hz, 4H). FAB-MS (*m/z*) (matrix: DTT/TG = 1:2): 453 ([*M* + 1]⁺, 100%). Anal. Calcd for C₂₂H₂₄N₄O₂F₄: C, 58.40; H, 5.35; N, 12.38. Found: C, 58.35; H, 5.39; N, 12.26.

Table 1. Crystal Data of Metal Complexes

	1a/AgCF ₃ SO ₃	2a/AgCF ₃ SO ₃	3a/AgCF ₃ SO ₃	4a/AgCF ₃ SO ₃
formula	C ₂₃ H ₂₈ AgF ₇ N ₄ O ₃ S	C ₂₃ H ₃₂ AgF ₃ N ₄ O ₃ S	C ₇₀ H ₈₀ Ag ₂ F ₆ N ₈ O ₁₀ S ₂	C ₄₈ H ₅₄ AgF ₃ N ₆ O ₄ S
<i>M</i>	681.42	609.46	1587.28	975.90
<i>T</i> /K	298	298	90	173
cryst syst	monoclinic	monoclinic	monoclinic	monoclinic
space group	<i>P</i> 2(1)/ <i>c</i>	<i>P</i> 2(1)/ <i>c</i>	<i>C</i> 2/ <i>c</i>	<i>P</i> 2(1)
<i>a</i> /Å	20.7362(19)	14.6799(8)	44.359(3)	10.1046(9)
<i>b</i> /Å	10.8673(10)	10.2113(6)	10.5230(5)	9.9420(8)
<i>c</i> /Å	12.0256(11)	16.6281(9)	33.2164(19)	22.717(2)
β /deg	100.386(2)	94.6660(10)	115.458(2)	99.837(2)
<i>U</i> /Å ³	2665.5(4)	2484.3(2)	13999.5(13)	2248.6(3)
<i>Z</i>	4	4	8	2
<i>D_c</i> /g cm ⁻³	1.698	1.629	1.506	1.441
μ /mm ⁻¹	0.917	0.951	0.699	0.559
data/restraints/params	6632/18/360	6177/0/324	17368/0/972	10191/2/576
no. reffs used [$>2\sigma(I)$]	6632 [<i>R</i> (int) = 0.0504]	6177 [<i>R</i> (int) = 0.0208]	17 368 [<i>R</i> (int) = 0.0609]	10 191 [<i>R</i> (int) = 0.0305]
<i>R₁</i> , <i>wR₂</i> [$I > 2\sigma(I)$]	0.0863, 0.1860	0.0436, 0.1134	0.0563, 0.1163	0.0665, 0.1756
<i>R₁</i> , <i>wR₂</i> [all data]	0.1264, 0.2089	0.0531, 0.1209	0.0858, 0.1273	0.0820, 0.1875
GOF	1.101	1.042	1.035	1.077
	5a/AgCF ₃ SO ₃	6a/AgCF ₃ SO ₃	7a/AgCF ₃ SO ₃	6a/HgCl ₂
formula	C ₃₁ H ₃₆ AgF ₃ N ₄ O ₃ S	C ₄₀ H ₄₄ AgF ₃ N ₄ O ₄ S	C ₄₄ H ₄₄ AgF ₃ N ₄ O ₄ S	C ₃₈ H ₄₀ HgCl ₂ N ₄
<i>M</i>	709.57	841.72	889.76	824.23
<i>T</i> /K	298	100	90	90
cryst syst	monoclinic	monoclinic	monoclinic	monoclinic
space group	<i>C</i> 2/ <i>c</i>	<i>P</i> 2(1)/ <i>c</i>	<i>C</i> <i>c</i>	<i>C</i> 2/ <i>c</i>
<i>a</i> /Å	13.298(2)	10.1283(7)	19.473(2)	22.1820(19)
<i>b</i> /Å	14.800(2)	19.0025(14)	16.4227(17)	7.6862(6)
<i>c</i> /Å	17.760(3)	19.4108(14)	14.1119(15)	20.9636(16)
β /deg	107.748(3)	94.6190(10)	117.169(2)	104.577(2)
<i>U</i> /Å ³	3329.0(9)	3723.7(5)	4015.1(7)	3459.1(5)
<i>Z</i>	4	4	4	4
<i>D_c</i> /g cm ⁻³	1.416	1.501	1.472	1.583
μ /mm ⁻¹	0.721	0.660	0.617	4.637
data/restraints/params	4165/12/235	9217/7/486	9300/53/519	4305/0/209
no. reffs used [$>2\sigma(I)$]	4165 [<i>R</i> (int) = 0.0468]	9217 [<i>R</i> (int) = 0.0232]	9300 [<i>R</i> (int) = 0.0285]	4305 [<i>R</i> (int) = 0.0476]
<i>R₁</i> , <i>wR₂</i> [$I > 2\sigma(I)$]	0.1150, 0.2698	0.0461, 0.1179	0.0737, 0.1960	0.0515, 0.1420
<i>R₁</i> , <i>wR₂</i> [all data]	0.1300, 0.2769	0.0501, 0.1207	0.0856, 0.2104	0.0521, 0.1424
GOF	1.393	1.102	1.043	1.185
	7a/Cu(CF ₃ SO ₃) ₂		5a	
formula	C ₄₄ H ₄₂ CuF ₆ N ₄ O ₇ S ₂		C ₃₀ H ₃₆ N ₄	
<i>M</i>	980.48		452.63	
<i>T</i> /K	90		298	
cryst syst	monoclinic		triclinic	
space group	<i>P</i> 2(1)/ <i>c</i>		$\bar{P}1$	
<i>a</i> /Å	12.9581(8)		11.5947(16)	
<i>b</i> /Å	16.6195(10)		14.973(2)	
<i>c</i> /Å	20.0520(11)		16.169(2)	
α /deg			81.717(3)	
β /deg	108.536(2)		78.957(2)	
γ /deg			68.798(3)	
<i>U</i> /Å ³	4094.3(4)		2560.0(6)	
<i>Z</i>	4		4	
<i>D_c</i> /g cm ⁻³	1.591		1.174	
μ /mm ⁻¹	0.722		0.070	
data/restraints/params	10184/0/593		12487/0/629	
no. reffs used [$>2\sigma(I)$]	10 184 [<i>R</i> (int) = 0.0737]		12 487 [<i>R</i> (int) = 0.0200]	
<i>R₁</i> , <i>wR₂</i> [$I > 2\sigma(I)$]	0.0613, 0.1211		0.0643, 0.1717	
<i>R₁</i> , <i>wR₂</i> [all data]	0.0979, 0.1354		0.1317, 0.2328	
GOF	1.026		1.028	

2b: Yield 85%. Mp: 135–136.5 °C. ^1H NMR (CDCl_3): δ 7.48–7.29 (m, 10H), 7.16 (s, 2H), 3.82 (s, 2H), 3.70 (s, 2H), 3.31–3.17 (m, 8H), 2.61 (t, $J = 5.7$ Hz, 4H). FAB-MS (m/z) (matrix: DTT/TG = 1:2): 381 ($[\text{M} + 1]^+$, 100%). Anal. Calcd for $\text{C}_{22}\text{H}_{28}\text{N}_4\text{O}_2$: C, 69.45; H, 7.42; N, 14.73. Found: C, 69.40; H, 7.40; N, 14.84.

3b: Yield 80%. Mp: 162.8–163.9 °C. ^1H NMR (CDCl_3): δ 7.35–7.31 (m, 4H), 7.28–7.24 (m, 4H), 7.13–7.07 (m, 6H), 7.02–6.96 (m, 8H), 3.78 (s, 2H), 3.65 (s, 2H), 3.25 (s, 8H), 2.62 (t, $J = 5.5$ Hz, 4H). FAB-MS (m/z) (matrix: DTT/TG = 1:2): 565 ($[\text{M} + 1]^+$, 30%). Anal. Calcd for $\text{C}_{34}\text{H}_{36}\text{N}_4\text{O}_4 + 0.5\text{SCH}_3\text{OH}$: C, 71.36; H, 6.60; N, 9.65. Found: C, 71.56; H, 6.41; N, 9.49.

4b: Yield 73%. Mp: 202.4–203.2 °C. ^1H NMR (CDCl_3): δ 7.23–7.17 (m, 10H), 7.14–7.11 (m, 4H), 7.01–6.96 (m, 16H), 3.73 (s, 2H), 3.61 (s, 2H), 3.27 (s, 4H), 3.23–3.22 (m, 4H), 2.63 (t, $J = 5.5$ Hz, 4H). FAB-MS (m/z) (matrix: DTT/TG = 1:2): 715 ($[\text{M} + 1]^+$, 2%). Anal. Calcd for $\text{C}_{46}\text{H}_{46}\text{N}_6\text{O}_2 + 0.25\text{H}_2\text{O}$: C, 76.80; H, 6.51; N, 11.68. Found: C, 76.83; H, 6.55; N, 11.65.

5b: Yield 43%. Mp: 132.6–133.0 °C. ^1H NMR (D_2O in the presence of NaOD): δ 8.30–8.37 (m, 2H), 8.00 (d, $J = 7.6$ Hz, 2H), 7.82–7.89 (m, 2H), 7.58–7.69 (m, 3H), 7.42–7.54 (s, 5H), 5.08 (s, 2H), 4.27 (s, 2H), 3.20–3.51 (m, 16H). FAB-MS (m/z) (matrix: DTT/TG = 1:2): 481 ($[\text{M} + 1]^+$, 100%). Anal. Calcd for $\text{C}_{30}\text{H}_{32}\text{N}_4\text{O}_2 + 0.5\text{SCHCl}_3$: C, 67.80; H, 6.06; N, 10.37. Found: C, 67.47; H, 6.32; N, 10.42.

6b: Yield 71%. Mp: 273.8–274.5 °C. ^1H NMR (CDCl_3): δ 8.53 (s, 1H), 8.41–8.39 (m, 2H), 8.24 (d, $J = 9.1$ Hz, 2H), 7.52–7.45 (m, 4H), 7.32 (t, $J = 6.6$ Hz, 2H), 8.42 (s, 1H), 8.09–8.06 (m, 2H), 7.97 (d, $J = 8.4$ Hz, 2H), 7.10 (t, $J = 6.6$ Hz, 2H), 6.69 (s, 2H), 4.80 (s, 2H), 4.64 (s, 2H), 3.27 (s, 4H), 2.99–2.95 (m, 4H), 2.62 (t, $J = 5.8$ Hz, 4H). FAB-MS (m/z) (matrix: DTT/TG = 1:2): 581 ($[\text{M} + 1]^+$, 20%). Anal. Calcd for $\text{C}_{38}\text{H}_{36}\text{N}_4\text{O}_2 + 0.5\text{SCH}_3\text{OH}$: C, 77.99; H, 6.29; N, 9.57. Found: C, 78.08; H, 6.34; N, 9.50.

7b: Yield 84%. Mp: 251.3–252.1 °C. ^1H NMR (CD_2Cl_2): δ 8.41 (d, $J = 9.5$ Hz, 1H), 8.33 (d, $J = 9.5$ Hz, 1H), 8.23 (d, $J = 6.9$ Hz, 1H), 8.17 (d, $J = 8.1$ Hz, 1H), 8.15–8.07 (m, 4H), 8.03–7.96 (m, 3H), 7.90 (t, $J = 7.7$ Hz, 1H), 7.87–7.85 (m, 2H), 7.82–7.76 (m, 3H), 7.54 (d, $J = 9.1$ Hz, 1H), 6.88 (s, 2H), 4.46 (s, 2H), 4.34 (s, 2H), 3.32 (s, 4H), 3.02–3.01 (m, 4H), 2.63 (t, $J = 5.8$ Hz, 4H). FAB-MS (m/z) (matrix: DTT/TG = 1:2): 629 ($[\text{M} + 1]^+$, 20%). Anal. Calcd for $\text{C}_{42}\text{H}_{36}\text{N}_4\text{O}_2$: C, 80.23; H, 5.77; N, 8.91. Found: C, 80.00; H, 5.88; N, 8.79.

General Procedure for Reduction of 4,10-Disubstituted-1,4,7,10-tetraazacyclododecane-2,12-diones. A mixture of **1b** (2.00 mmol) and DIBAL-H (40 mL, 1 mol/L solution in THF) was stirred for 1 day at room temperature. After benzene (120 mL), NaF (160 mmol), and water (2 mL) were added at 0 °C, the mixture was stirred a further day at room temperature under an argon atmosphere. The mixture was filtered, and the filtrate was evaporated under reduced pressure. The residual solid was recrystallized from acetonitrile to give **1a** in 70% yield. Mp: 157.1–158.2 °C. ^1H NMR (CD_2Cl_2): δ 6.91 (d, $J = 6.0$ Hz, 4H), 6.73 (tt, $J_1 = 9.1$ Hz, $J_2 = 2.4$ Hz, 2H), 3.59 (s, 4H), 2.63 (broad s, 8H), 2.56 (broad d, $J = 4.9$ Hz, 8H). ^{13}C NMR* (CD_2Cl_2): δ 163.4 (dd, $^1J_{\text{CF}} = 248.0$ and $^3J_{\text{CF}} = 12.7$ Hz), 144.4 (t, $^3J_{\text{CF}} = 8.5$ Hz), 112.0 (dd, $^2J_{\text{CF}} = 24.4$ Hz and $^4J_{\text{CF}} = 6.2$ Hz), 102.7 (t, $^2J_{\text{CF}} = 25.5$ Hz), 59.6, 52.2, 45.6. FAB-MS (m/z) (matrix: DTT/TG = 1:2): 425 ($[\text{M} + 1]^+$, 100%). Anal. Calcd for $\text{C}_{22}\text{H}_{28}\text{N}_4\text{F}_4$: C, 62.25; H, 6.65; N, 13.20. Found: C, 62.32; H, 6.75; N, 13.22. *Signs of ^{13}C – ^{19}F coupling constants in the ^{13}C NMR spectrum of **1a** have not been considered.

2a: Yield 56%. Mp: 200.0–201.0 °C. ^1H NMR (CD_2Cl_2): δ 7.25–7.42 (m, 10H), 3.56 (s, 4H), 2.56–2.64 (m, 18H). ^{13}C NMR (CD_2Cl_2): δ 140.26, 129.6, 128.6, 127.4, 60.3, 52.1, 45.6. FAB-MS (m/z) (matrix: DTT/TG = 1:2): 353 ($[\text{M} + 1]^+$, 100%). Anal. Calcd for $\text{C}_{22}\text{H}_{32}\text{N}_4$: C, 74.96; H, 9.15; N, 15.89. Found: C, 75.09; H, 9.19; N, 13.90.

3a: Yield 45%. Mp: 98.5–100.2 °C. ^1H NMR (CD_2Cl_2): δ 7.24–7.35 (m, 8H), 7.07 (t, $J = 7.3$ Hz, 2H), 6.91–7.02 (m, 8H), 3.53 (s, 4H), 2.49–2.65 (m, 18H). ^{13}C NMR (CD_2Cl_2): δ 157.7, 156.7, 135.0, 130.8, 130.1, 123.6, 119.2, 118.9, 59.4, 52.1, 45.6. FAB-MS (m/z) (matrix: DTT/TG = 1:2): 537 ($[\text{M} + 1]^+$, 20%). Anal. Calcd for

$\text{C}_{34}\text{H}_{40}\text{N}_4\text{O}_2$: C, 76.09; H, 7.51; N, 10.44. Found: C, 76.14; H, 7.53; N, 10.39.

4a: Yield 77%. Yellow oil. ^1H NMR (CD_2Cl_2): δ 7.13–7.23 (m, 12H), 6.91–7.03 (m, 16H), 3.53 (s, 4H), 2.51–2.69 (m, 18H). ^{13}C NMR (CD_2Cl_2): δ 148.3, 147.1, 134.4, 130.3, 129.6, 124.38, 124.36, 123.0, 59.7, 52.1, 45.9. FAB-MS (m/z) (matrix: DTT/TG = 1:1): 687 ($[\text{M} + 1]^+$, 20%). Anal. Calcd for $\text{C}_{46}\text{H}_{50}\text{N}_6 + \text{H}_2\text{O}$: C, 78.37; H, 7.43; N, 11.92. Found: C, 78.25; H, 7.38; N, 11.63.

5a: Yield 43%. Mp: 134.0–134.8 °C. ^1H NMR (CD_2Cl_2): δ 8.14–8.20 (m, 2H), 7.85–7.91 (m, 2H), 7.80 (d, $J = 8.1$ Hz, 2H), 7.40–7.57 (m, 8H), 4.01 (s, 4H), 2.63 (s, 16H). ^{13}C NMR (CD_2Cl_2): δ 135.3, 134.2, 132.8, 129.0, 128.0, 127.8, 126.4, 125.9, 125.8, 124.1, 58.2, 52.7, 45.8. FAB-MS (m/z) (matrix: DTT/TG = 1:1): 687 ($[\text{M} + 1]^+$, 20%). Anal. Calcd for $\text{C}_{30}\text{H}_{36}\text{N}_4$: C, 79.60; H, 8.02; N, 12.38. Found: C, 79.38; H, 8.05; N, 12.42.

6a: Yield 69%. Mp: 223.5–224.9 °C. ^1H NMR (CD_2Cl_2): δ 8.47 (s, 2H), 8.28 (d, $J = 9.0$ Hz, 4H), 8.04 (d, $J = 8.5$ Hz, 4H), 7.47 (t, $J = 7.6$ Hz, 4H), 7.21 (t, $J = 7.6$ Hz, 4H), 4.42 (s, 4H), 2.63 (d, $J = 8.1$ Hz, 16H). ^{13}C NMR (CD_2Cl_2): δ 132.0, 131.8, 130.0, 130.3, 128.0, 126.6, 125.4, 124.9, 52.9, 52.4, 45.7. FAB-MS (m/z) (matrix: DTT/TG = 1:2): 553 ($[\text{M} + 1]^+$, 100%). Anal. Calcd for $\text{C}_{38}\text{H}_{40}\text{N}_4$: C, 82.57; H, 7.29; N, 10.14. Found: C, 82.24; H, 7.26; N, 10.09.

7a: Yield 28%. Mp: 165.2–166.1 °C (dec). ^1H NMR (CD_2Cl_2): δ 8.45 (d, $J = 9.3$ Hz, 2H), 8.21 (d, $J = 7.5$ Hz, 2H), 7.90–8.14 (m, 14H), 4.28 (s, 4H), 2.55–2.73 (m, 16H). ^{13}C NMR (CD_2Cl_2): δ 133.6, 131.8, 131.2, 130.9, 130.0, 128.5, 127.9, 127.8, 127.4, 126.3, 125.5, 125.4, 125.24, 125.23, 125.1, 123.7, 58.3, 52.9, 46.0. FAB-MS (m/z) (matrix: DTT/TG = 1:2): 601 ($[\text{M} + 1]^+$, 50%). Anal. Calcd for $\text{C}_{42}\text{H}_{40}\text{N}_4$: C, 83.96; H, 6.71; N, 9.33. Found: C, 84.02; H, 6.83; N, 9.20.

Preparation of Metal Ion Complexes. The ligand (0.0151 mmol) in chloroform (1 mL) was added to the corresponding metal salt (AgOTf , $\text{Cu}(\text{OTf})_2$, or HgCl_2) (0.0153 mmol) in methanol (1 mL). Crystals were obtained quantitatively on evaporation of the solvent.

1a/AgOTf. Anal. Calcd for $\text{C}_{23}\text{H}_{28}\text{N}_4\text{F}_7\text{O}_3\text{SAg}$: C, 40.54; H, 4.14; N, 8.22. Found: C, 40.64; H, 3.66; N, 7.95.

2a/AgOTf. Anal. Calcd for $\text{C}_{23}\text{H}_{32}\text{N}_4\text{F}_3\text{O}_3\text{SAg}$: C, 45.33; H, 5.29; N, 9.19. Found: C, 45.15; H, 5.41; N, 8.95.

3a/AgOTf. Anal. Calcd for $\text{C}_{35}\text{H}_{40}\text{N}_4\text{F}_3\text{O}_3\text{SAg}$: C, 52.97; H, 5.08; N, 7.06. Found: C, 53.06; H, 5.02; N, 7.01.

4a/AgOTf. Anal. Calcd for $\text{C}_{47}\text{H}_{50}\text{N}_6\text{F}_3\text{O}_3\text{SAg}$: C, 59.81; H, 5.34; N, 8.90. Found: C, 59.67; H, 5.18; N, 8.85.

5a/AgOTf. Anal. Calcd for $\text{C}_{31}\text{H}_{36}\text{N}_4\text{F}_3\text{O}_3\text{SAg} + 0.8\text{CHCl}_3$: C, 47.44; H, 4.61; N, 6.96. Found: C, 47.39; H, 4.29; N, 6.96.

6a/AgOTf. Anal. Calcd for $\text{C}_{39}\text{H}_{40}\text{N}_4\text{F}_3\text{O}_3\text{SAg} + 0.6\text{CHCl}_3$: C, 53.97; H, 4.64; N, 6.36. Found: C, 54.07; H, 4.62; N, 6.42.

7a/AgOTf. Anal. Calcd for $\text{C}_{43}\text{H}_{40}\text{N}_4\text{F}_3\text{O}_3\text{SAg} + 0.1\text{CHCl}_3$: C, 59.53; H, 4.65; N, 6.44. Found: C, 59.28; H, 4.42; N, 6.46.

7a/CuOTf₂. Anal. Calcd for $\text{C}_{44}\text{H}_{40}\text{N}_4\text{F}_6\text{O}_6\text{S}_2\text{Cu}$: C, 54.91; H, 4.19; N, 5.82. Found: C, 54.94; H, 3.93; N, 5.73.

6a/HgCl₂. Anal. Calcd for $\text{C}_{38}\text{H}_{40}\text{N}_4\text{Cl}_2\text{Hg} + 1.3\text{CHCl}_3$: C, 48.19; H, 4.25; N, 5.72. Found: C, 48.27; H, 4.22; N, 5.92.

Crystals of the metal complexes with **1a**–**7a** were mounted on top of a glass fiber, and data collections were performed using a Bruker SMART CCD area diffractometer at 90–223 K. Data were corrected for Lorentz and polarization effects, and absorption corrections were applied using the SADABS¹⁰ program. Structures were solved by a direct method and subsequent difference-Fourier syntheses using the program SHELEX.¹¹ All non-hydrogen atoms were refined anisotropically, and hydrogen atoms were placed at calculated positions and then refined using $U_{\text{iso}}(\text{H}) = 1.2U_{\text{eq}}(\text{C})$. The crystallographic refinement parameters of the complexes are summarized in Table 1.

■ ASSOCIATED CONTENT

Supporting Information

Spectral data and titration experiments (PDF). Crystallographic data of metal complexes with **1a**–**7a** (CIF). These materials are available free of charge via the Internet at <http://pubs.acs.org>

AUTHOR INFORMATION

Corresponding Author

*E-mail: habata@chem.sci.toho-u.ac.jp.

Notes

The authors declare no competing financial interest.

ACKNOWLEDGMENTS

This research was supported by Grants-in-Aid (08026969 and 11011761), a High-Tech Research Center project (2005–2009), and the Supported Program for Strategic Research Foundation at Private Universities (2012–2016) from the Ministry of Education, Culture, Sports, Science and Technology of Japan, and the Futaba Memorial Foundation, for Y.H.

DEDICATION

This paper is dedicated to the late Professor Sadatoshi Akabori, who passed away on October 3, 2012.

REFERENCES

- (1) (a) Gokel, G. W. *Chem. Commun.* **2003**, 2847. (b) Gokel, G. W.; Barbour, L. J.; De, W. S. L.; Meadows, E. S. *Coord. Chem. Rev.* **2001**, *222*, 127. (c) Gokel, G. W.; De, W. S. L.; Meadows, E. S. *Eur. J. Org. Chem.* **2000**, 2967. (d) Petrella, A. J.; Raston, C. L. *J. Organomet. Chem.* **2004**, *689*, 4125. (e) Xu, Z. *Coord. Chem. Rev.* **2006**, *250*, 2745. (f) Zaric, S. D. *Eur. J. Inorg. Chem.* **2003**, 2197. (g) Munakata, M.; Wu, L. P.; Ning, G. L. *Coord. Chem. Rev.* **2000**, *198*, 171.
- (2) (a) Abe, M.; Eto, M.; Yamaguchi, K.; Yamasaki, M.; Misaka, J.; Yoshitake, Y.; Otsuka, M.; Harano, K. *Tetrahedron* **2012**, *68*, 3566. (b) Krenske, E. H.; Houk, K. N. *Acc. Chem. Res.* Ahead of Print. (c) Nishio, M. *Tetrahedron* **2005**, *61*, 6923. (d) Nishio, M. *CrystEngComm* **2004**, *6*, 130. (e) Nishio, M.; Umezawa, Y.; Hirota, M.; Takeuchi, Y. *Tetrahedron* **1995**, *51*, 8665.
- (3) Baudron, S. A. *CrystEngComm* **2010**, *12*, 2288. Beziau, A.; Baudron, S. A.; Hosseini, M. W. *Dalton Trans.* **2012**, *41*, 7227. Chainok, K.; Neville, S. M.; Forsyth, C. M.; Gee, W. J.; Murray, K. S.; Batten, S. R. *CrystEngComm* **2012**, *14*, 3717. Gao, C.-Y.; Zhao, L.; Wang, M.-X. *J. Am. Chem. Soc.* **2012**, *134*, 824. Goodgame, D. M. L.; Grachvogel, D. A.; Williams, D. J. *J. Chem. Soc., Dalton Trans.* **2002**, 2259. Guney, E.; Yilmaz, V. T.; Buyukgungor, O. *Inorg. Chem. Commun.* **2010**, *13*, 563. Hamamci, S.; Yilmaz, V. T.; Buyukgungor, O. *Acta Crystallogr. C* **2006**, *62*, m1. Hao, H.-J.; Sun, D.; Li, Y.-H.; Liu, F.-J.; Huang, R.-B.; Zheng, L.-S. *Cryst. Growth Des.* **2011**, *11*, 3564. Ino, I.; Wu, P.; Munakata, M.; Kuroda-Sowa, T.; Maekawa, M.; Suenaga, Y.; Sakai, R. *Inorg. Chem.* **2000**, *39*, 5430. Kennedy, A. R.; Brown, K. G.; Graham, D.; Kirkhouse, J. B.; Kittner, M.; Major, C.; McHugh, C. J.; Murdoch, P.; Smith, W. E. *New J. Chem.* **2005**, *29*, 826. Khanna, S.; Verma, S. *Cryst. Growth Des.* **2012**, *12*, 3025. Kim, S. K.; Lee, J. K.; Lee, S. H.; Lim, M. S.; Lee, S. W.; Sim, W.; Kim, J. S. *J. Org. Chem.* **2004**, *69*, 2877. Lahtinen, T.; Wegelius, E.; Rissanen, K. *New J. Chem.* **2001**, *25*, 905–911. Li, B.; Zang, S.-Q.; Li, H.-Y.; Wu, Y.-J.; Mak, T. C. W. *J. Organomet. Chem.* **2012**, *708–709*, 112. Li, X. Y.; Liu, Q. K.; Ma, J. P.; Huang, R. Q.; Dong, Y. B. *Acta Crystallogr. C* **2009**, *65*, m45. Liddle, B. J.; Hall, D.; Lindeman, S. V.; Smith, M. D.; Gardinier, J. R. *Inorg. Chem.* **2009**, *48*, 8404. Lindeman, S. V.; Rathore, R.; Kochi, J. K. *Inorg. Chem.* **2000**, *39*, 5707. Liu, H.-K.; Huang, X.; Lu, T.; Wang, X.; Sun, W.-Y.; Kang, B.-S. *Dalton Trans.* **2008**, 3178. Luo, G.-G.; Xiong, H.-B.; Sun, D.; Wu, D.-L.; Huang, R.-B.; Dai, J.-C. *Cryst. Growth Des.* **2011**, *11*, 1948. Munakata, M.; Ning, G. L.; Suenaga, Y.; Kuroda-Sowa, T.; Maekawa, M.; Ohta, T. *Angew. Chem., Int. Ed.* **2000**, *39*, 4555. Munakata, M.; Wen, M.; Suenaga, Y.; Kuroda-Sowa, T.; Maekawa, M.; Anahata, M. *Polyhedron* **2001**, *20*, 2321. Reger, D. L.; Gardinier, J. R.; Smith, M. D. *Inorg. Chem.* **2004**, *43*, 3825. Richards, P. I.; Steiner, A. *Inorg. Chem.* **2004**, *43*, 2810. Santra, R.; Banerjee, K.; Biradha, K. *Chem. Commun.* **2011**, 47, 10740. Son, J.-H.; Pudenz, M. A.; Hoefelmeyer, J. D. *Dalton Trans.* **2010**, 39, 11081. Sumby, C. J.; Steel, P. J. *Inorg. Chim. Acta* **2007**, *360*, 2100. Sun, D.; Luo, G.-G.; Xu, Q.-J.; Zhang, N.; Jin, Y.-C.; Zhao, H.-X.; Lin, L.-R.; Huang, R.-B.; Zheng, L.-S. *Inorg. Chem. Commun.* **2009**, *12*, 782. Sun, D.; Zhang, N.; Luo, G. G.; Huang, R. B.; Zheng, L. S. *Acta Crystallogr. C* **2010**, *C66*, m75. Sun, D.; Zhang, N.; Xu, Q.-J.; Huang, R.-B.; Zheng, L.-S. *J. Organomet. Chem.* **2010**, *695*, 1598. Tan, H.-Y.; Zhang, H.-X.; Ou, H.-D.; Kang, B.-S. *Inorg. Chim. Acta* **2004**, *357*, 869. Trzebuniak, K.; Zarychta, B.; Olijnyk, V. *J. Mol. Struct.* **2011**, *1006*, 266. Wadepohl, H.; Pritzkow, H. *Acta Crystallogr.* **2001**, *C57*, 383. Wang, F. Y.; Jiang, X. B.; Tan, X. J.; Xing, D. X. *Acta Crystallogr.* **2011**, *C67*, 218. Wen, M.; Munakata, M.; Suenaga, Y.; Kuroda-Sowa, T.; Maekawa, M. *Inorg. Chim. Acta* **2002**, *332*, 18. Wen, Q.-S.; Zhou, C.-L.; Qin, D.-B. *Acta Crystallogr.* **2010**, *E66*, m1030. Yesilel, O. Z.; Guenay, G.; Buyukgungor, O. *Polyhedron* **2011**, *30*, 364. Zang, S.-Q.; Han, J.; Mak, T. C. W. *Organometallics* **2009**, *28*, 2677. Zhao, L.; Mak, T. C. W. *Organometallics* **2007**, *26*, 4439. Zhao, L.; Zhao, X.-L.; Mak, T. C. W. *Chem.–Eur. J.* **2007**, *13*, 5927. Zheng, S. L.; Tong, M. L.; Tan, S. D.; Wang, Y.; Shi, J. X.; Tong, Y. X.; Lee, H. K.; Chen, X. M. *Organometallics* **2001**, *20*, 5319. Zheng, S.-L.; Zhang, J.-P.; Wong, W.-T.; Chen, X.-M. *J. Am. Chem. Soc.* **2003**, *125*, 6882. Zheng, X.-F.; Zhu, L.-G. *Cryst. Growth Des.* **2009**, *9*, 4407. Zheng, X.-F.; Zhu, L.-G. *Inorg. Chim. Acta* **2011**, *365*, 419. Zhong, J. C.; Munakata, M.; Kuroda-Sowa, T.; Maekawa, M.; Suenaga, Y.; Konaka, H. *Inorg. Chem.* **2001**, *40*, 3191. Zhou, Y.; Zhang, X.; Chen, W.; Qiu, H. *J. Organomet. Chem.* **2008**, *693*, 205.
- (4) (a) Habata, Y.; Ikeda, M.; Yamada, S.; Takahashi, H.; Ueno, S.; Suzuki, T.; Kuwahara, S. *Org. Lett.* **2014**, *14*, 4576. (b) Habata, Y.; Okeda, Y.; Ikeda, M.; Kuwahara, S. Submitted.
- (5) Neuburger, M.; Zehnder, M.; Kaden, T. A. *Supramol. Chem.* **1993**, *2*, 103. DeSimone, R. E.; Blinn, E. L.; Mucker, K. F. *Inorg. Nucl. Chem. Lett.* **1980**, *16*, 23. Kobayashi, K.; Sakurai, T.; Hasegawa, A.; Tsuboyama, S.; Tsuboyama, K. *Acta Crystallogr.* **1982**, *B38*, 1154. Kong, D.-Y.; Xie, Y.-L.; Xie, Y.-Y.; Huang, X.-Y. *Jiegou Huaxue* **2000**, *19*, 39. Kong, D.; Huang, X.; Xie, Y. *Inorg. Chim. Acta* **2002**, *340*, 133. Kong, D.; Meng, L.; Song, L.; Xie, Y. *Transition Met. Chem.* **1999**, *24*, 553. Sakurai, T.; Tsuboyama, K.; Tsuboyama, S.; Kobayashi, K. *Nippon Kessho Gakkaishi* **1983**, *25*, 299. Sakurai, T.; Kobayashi, K.; Hasegawa, A.; Tsuboyama, S.; Tsuboyama, K. *Acta Crystallogr.* **1982**, *B38*, 107. Sakurai, T.; Kobayashi, K.; Kanari, T.; Kawata, T.; Higashi, I.; Tsuboyama, S.; Tsuboyama, K. *Acta Crystallogr.* **1983**, *B39*, 84. Sakurai, T.; Kobayashi, K.; Masuda, H.; Tsuboyama, S.; Tsuboyama, K. *Acta Crystallogr.* **1983**, *C39*, 334. Tsuboyama, S.; Kobayashi, K.; Sakurai, T.; Tsuboyama, K. *Acta Crystallogr.* **1984**, *C40*, 1178. Tsuboyama, S.; Saitoh, N.; Kobayashi, K.; Tsuboyama, K.; Sakurai, T. *Anal. Sci.* **1989**, *5*, 115.
- (6) “Argentivorous” is different from “argentophilic”. “Argentophilic” is used in the sense of Ag⁺–Ag⁺ interactions. For example: (a) Constable, E. C.; Housecroft, C. E.; Kopecky, P.; Neuburger, M.; Zampese, J. A. *Inorg. Chem. Commun.* **2013**, *27*, 159–162. (b) Luo, G.-G.; Wu, D.-L.; Liu, L.; Wu, S.-H.; Li, D.-X.; Xiao, Z.-J.; Dai, J.-C. *J. Mol. Struct.* **2012**, *1014*, 92–96. (c) Santra, R.; Garai, M.; Mondal, D.; Biradha, K. *Chemistry* **2013**, *19*, 489–93. (d) Senchyk, G. A.; Bukhan'ko, V. O.; Lysenko, A. B.; Krautscheid, H.; Rusanov, E. B.; Chernega, A. N.; Karbowski, M.; Domasevitch, K. V. *Inorg. Chem.* **2012**, *51*, 8025–8033. (e) Stephenson, A.; Ward, M. D. *Chem. Commun. (Cambridge, U. K.)* **2012**, 48, 3605–3607. (f) Xu, J.; Gao, S.; Ng, S. W.; Tiekink, E. R. T. *Acta Crystallogr., Sect. E Struct. Rep. Online* **2012**, *68*, m639–40. (g) Xu, J.; Gao, S.; Ng, S. W.; Tiekink, E. R. T. *Acta Crystallogr., Sect. E Struct. Rep. Online* **2012**, *E68*, m639–m640. (h) Yang, G.; Baran, P.; Martinez, A. R.; Raptis, R. G. *Cryst. Growth Des.* **2013**, *13*, 264–269.
- (7) 1,4,7,10-Tetraazacyclododecane-2,6-dione was prepared according to the procedure described in the following literature: Kodama, M.; Kimura, E. *J. Chem. Soc., Dalton Trans.* **1981**, *3*, 694. Compounds **2a**, **5a**, and **6a** have been prepared in different procedures. **2a**: Chaux, F.; Denat, F.; Espinosa, E.; Guillard, R. *Chem. Commun.* **2006**, 5054. Compound **5a**: Kikuta, E.; Murata, M.; Katsube, N.; Koike, T.; Kimura, E. *J. Am. Chem. Soc.* **1999**, *121*, 5426. Compound **6a**: Shiraiishi, Y.; Kohno, Y.; Hirai, T. *Ind. Eng. Chem. Res.* **2005**, *44*, 847.
- (8) *Spartan '10*; Wavefunction, Inc.: Irvine, CA.

(9) Hehre, W. J.; Yu, J.; Klunzinger, P. E.; Lou, L. *A Brief Guide to Molecular Mechanics and Quantum Chemistry Calculations*; Wavefunction: Irvine, CA, 1998; p 159.

(10) Sheldrick, G. M. *SADABS, Program for Adsorption Correction of Area Detector Frames*; Bruker AXS, Inc.: Madison, WI, 1996.

(11) *SHELXTLTM*, version 5.1; Bruker AXS, Inc.: Madison, WI, 1997.